Pre-print version final paper found at:
https://www.jstage.jst.go.jp/article/ieejjia/3/2/3_86/_pdf

Review Paper

A Review of Saliency-based Sensorless Control Methods for Alternating Current Machines

Cyril Spiteri Staines*a), Member, Cedric Caruana*, Non Member, Reiko Raute* Non Member

(Manuscript received Jan. 00, 20XX, revised May 00, 20XX)

Operation of model-based sensorless control of Alternating Current machines at low and zero speeds is unreliable and can fail. To overcome the limitations of sensorless control at low speeds, several alternative techniques have been developed to estimate speed and position. These are mainly based on detecting machine saliencies by measuring the response of the current to some form of voltage injection. This paper discusses injection methods, machine saliencies, and techniques used to extract speed and position that are applicable to both induction machines and permanent magnet synchronous motors.

Keywords : sensorless speed and position control, AC machines, signal injection, machine saliencies, hybrid system, PWM based injection.

1. Introduction

Model-based speed estimation in Alternating Current (AC) drives is possible at nearly all speeds, however most model based methods fail at low or zero speed. The reason is that their speed estimation fundamentally depends on determining the back-electromotive force (emf) or machine flux. At low speed, the back-emf decreases to an extent that noise, inaccuracies in sampled variables and inexact knowledge of the machine parameters yield relatively large estimation errors. In this respect, other methods independent of machine and inverter parameters aimed at estimating the rotor or flux position were developed. Machine parameter independent estimation at zero and low speeds is possible by employing tracking of a form of saliency in a machine to derive the flux or rotor position. In the case of asynchronous machines, the saliency could be due to the rotating flux itself [18] or the rotor slots [11,13,19,27] or a specially engineered rotor [3,4,5,6,8]. In the case of synchronous machines, the saliency is mainly caused by the magnetic saturation effect on surface permanent magnet synchronous motors [14,21,22,25] and/or the geometric saliency on interior permanent magnet synchronous motors [15,26].

Additional signal injection for saliency detection can be categorized into two types; transient and continuous. Moreover, recently methods to detect saliencies excited by selected switching states present in the inverter's inherent Pulse Width Modulation (PWM) switching or by the PWM's switching frequency itself have been introduced. This paper shall review a number of sensorless methods applied to both asynchronous and synchronous motors.

The methods employing transient and continuous injection were both developed during the 90s [1,4,5,6,10]. The transient injection method [1], better known as the INFORM method, estimates the flux angle by applying a transient test voltage and calculating the leakage inductance which varies due to the main path and leakage (slot) saturation. Later on other transient techniques, usually based on the measurement of current or voltage response to a sequence of test vectors, were developed. The concept originated from the work in [3] which introduced a technique which modified slightly the fundamental PWM switching by extending the duration of selected inherent switching vectors. When applied to a star connected induction machine (IM) the resulting voltage transients were used to derive rotor slot position dependent signals which could be used to track the rotor position at low and zero speed. In [18] this technique was extended to a delta connected machine and measurement of the resulting current derivatives yielded rotor flux position dependent signals which were used for flux tracking.

Concurrently whilst research was being carried out on the transient based techniques, research on improving methods based on continuous HF voltage injection was ongoing. The HF-based methods [2,4,5,6,7,16] employ a continuous injection signal and an observer for saliency tracking. The type of saliency present in the machine shall determine whether rotor or flux position-dependent HF harmonics shall result. By appropriate signal processing techniques, these harmonics can be used to yield the required position by configuring the observer to track magnetic flux [2,4] or physical saliencies [5,6,11]. Rotor "flux tracking" based methods yield parameter–independent flux position (if the machine is sufficiently saturated) which yields good low speed torque and flux control. For sensorless position and speed control at zero and low speeds a 'trackable' rotor position dependent saliency is required. This can be the natural saliency due to rotor slotting [11,13,27] or a designed rotor asymmetry [3,4,6]. The first rotors tested with high frequency injection consisted of engineered rotors such as those shown in Fig.1 [4] and Fig.2 [6]. Figs 1 and 2 show the periodic variation of the physical rotor circuit over one pole pitch which results in the sinusoidal variation of the leakage inductance and the rotor resistance respectively.

Another type of inherent rotor position saliency is caused by the interaction of the stator and rotor slots and it can be shown [13,11,27] that the permanence variation thus caused during operation rotates at a multiple of the actual rotor speed. Main and leakage flux saturation shall cause modulation of the local inductance introducing another type of saliency in the machine. This saliency can have a detrimental effect on methods employed in induction machines which use a rotor position 'trackable' anisotropy (rotor asymmetry) since it will result in multiple

a) Correspondence to: cyril.spiteri-staines@um.edu.mt
* University of Malta
Faculty of Engineering, , Msida, MSD 2080, Malta

saliencies [3,8,11]. In this respect, methods capable to take into account multiple saliences or to mitigate their effects were developed [8,11].

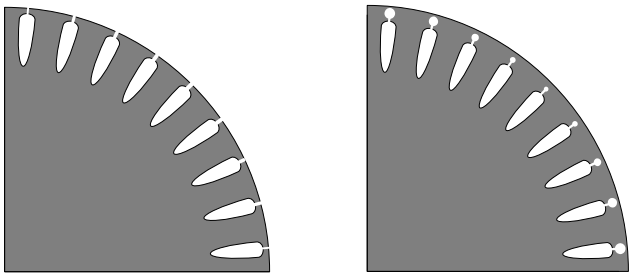

(a) (b)

Fig. 1 (a) Periodic variation of squirrel cage rotor slot openings, b) Periodic variation of Double Cage outer resistance.

The saliencies which exist in Permanent Magnet Synchronous Machines (PMSM)s differ from the above and can be of two types depending on whether the magnets are surface mounted or of the interior type. In the latter case, the saliency is a physical property of the machine due to the magnets' integration into the rotor. The Interior Magnet synchronous machines (IPMSM) lend themselves naturally for tracking of the rotor position due to their inherent saliency. In the case of the Surface Mount (SM) -PMSMs the saliency of the magnets themselves is very low; in fact they are considered to be non-salient. However in this case a saturation dependent saliency, which modulates the machine's inductances, is set-up by variation of the iron saturation of the stator teeth due to the rotor's permanent magnets' high flux density.

This paper shall look at various saliency based techniques used for sensorless speed/position estimation. It shall also discuss the hybrid concept for sensorless control, which incorporates both injection-based and model-based estimation, based on the principle that the injection method shall be employed only at speeds where the model-based estimation fails. Finally, the paper shall also review relatively new 'injection' methods based on the use of the inherent PWM switching which serves as the saliency excitation mechanism.

2. Continuous HF Injection for Tracking Saliencies

2.1 Concept of HF Injection

The control structure of Fig. 2 shows the system block diagram used for sensorless speed or position control. For the case of the continuous HF injection technique, the HF carrier voltage injected at 'ω_c' is :

$$u^s_{s\alpha\beta\_c}(t) = U_c e^{j\omega_c t} \quad \text{.....(1)}$$

In an IM, the leakage inductances, l_σ vary sinusoidally with respect to both the flux and rotor angle under the effects of main-flux/tooth saturation and rotor slotting respectively. Considering both effects, we have:

$$l_{\sigma\_x} = l_\sigma - \Delta l_{\sigma\_sat}\cos(2\omega_e t - k.2\pi/3) - \Delta l_{\sigma\_RS}\cos(n\omega_r t - k.2\pi/3 + \phi) \quad \text{.....(2)}$$

where, phase *'x'* corresponds to phase *'a','c','b'* for *k=0,1,2* respectively. l_σ is the average inductance per phase and Δl_{σ_sat} and Δl_{σ_RS} are the change in leakage inductance caused by saturation and rotor slotting respectively. For the case of a designed leakage asymmetry (such as shown in Fig. 1) and a low slotting effect, Δl_{σ_RS} would be replaced with Δl_{σ_ASY} and *n=2*.

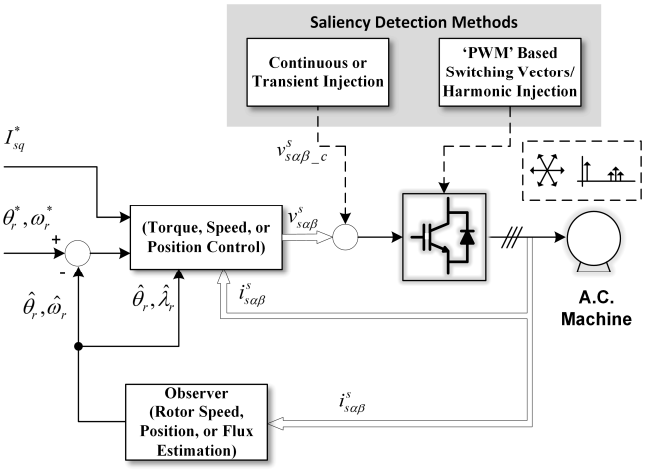

Fig. 2. Sensorless Control System.

When modeling the HF behavior, it can be shown that for the inductance variation of (2) the resulting HF stator currents for IM are given by (3) below. Similarly for a PMSM these are given by (4) below.

1.1.1 *Resultant HF current for an asynchronous machine including saturation-dependent harmonics.*

$$i^s_{s\alpha\beta\_c}(t) = I_1 e^{j(\omega_c t+\phi_1)} + I_2 e^{j(n\theta_r - \omega_c t - \phi_2)} + I_3 e^{j(2\theta_e - \omega_c t - \phi_3)} \quad \text{....(3)}$$

where: I_1 is the un-modulated resultant HF current; I_2 is the rotor asymmetry dependent HF component (*n=2* for a sinusoidally distributed rotor asymmetry over one pole pitch and weak rotor slotting, *n=number of rotor slots per pole* for a rotor slotting asymmetry and no designed asymmetry); I_3 is the saturation saliency dependent HF component; θ_r is the rotor position and θ_e is the flux saliency angle.

1.1.2 *Resultant HF current for an PM synchronous machine*

$$i^s_{s\alpha\beta\_c}(t) = I_1 e^{j(\omega_c t+\phi_1)} + I_2 e^{j(2\theta_\delta - \omega_c t - \phi_2)} \quad \text{.....(4)}$$

where: I_1 is as above; I_2 is the saturation saliency dependent HF component; θ_δ is the flux saliency position.
(In (3) and (4) $\phi_{1,2,3}$ are arbitrary phase angles).

Using a heterodyning based technique [4,6] or by transforming the resulting HF currents to a 'ω_c' frame and filtering [11,14], in the case of IMs, the components I_1 and I_3 can be extracted from (3) whilst in the case of PMSMs, component I_2 can be extracted from (4). This is shown in the demodulation block of Fig. 4.

2.2 Multiple Saliences in Induction Machines

Equation (2), shows the modulation of the local inductance in an IM due to main and leakage flux saturation. The saturation saliency can have a detrimental effect on methods which use a 'trackable' rotor asymmetry for position estimation since it will result in multiple saliencies [3,8,11]. For successful rotor position estimation, either :

1. the rotor asymmetry needs to be designed in such a manner so as to yield a position-dependent harmonic which under all operating conditions is larger than the other HF saliency harmonics, or
2. the estimation method has got to be capable of taking into account multiple saliency effects.

2.3 Rotor Flux Saliency position shift due to Load

The SM-PMSM machine is normally considered non-salient, however its rotor flux can still be tracked due to the modulation this flux causes in the machine's inductance. Unlike for the interior magnet PMSM, whose saliency is very pronounced, it was reported that the saliency axis in the surface mount machines does not correspond exactly with the rotor position [14]. Although they are nearly aligned, a phase shift that is a function of the machine load occurs between these two axes. This effect was even observed in IMs when employing sensorless flux tracking [18]. Such a characteristic is shown in Fig. 3 for an 11kW, 4-pole, three phase induction machine.

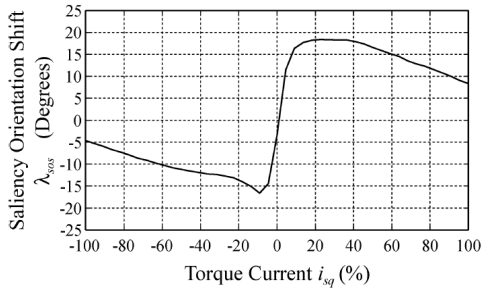

Fig. 3 Saliency orientation shift between the detected saliency angle and the true rotor flux angle.

2.4 Corrupting Harmonics and Mitigation Techniques

A possible solution to suppress the deteriorating effect of the saturation-dependent HF harmonics (at $2f_e$ and multiples) on rotor asymmetry based sensorless methods is to implement a compensation scheme as shown in Fig. 4. Assuming HF injection and only one saliency to be present, the resulting HF signal $i^s_{sdq\_c}$ will then contain the *sin* and *cos* of the saliency position angle. In practice however there will be additional parasitic saliencies together with the dominant saliency. One technique called the *Harmonic Compensation (HC)* was developed to compensate for such additional 'disturbing' harmonics [11]. This technique has been shown to be effective if only a small number of harmonics have to be suppressed. In a practical electric drive system the inverter introduces non-linearities due to deadtime and device voltage drop, these can introduce significant distortions in the HF signals. Thus a more comprehensive compensation technique which corrects for both 'corrupting' harmonics and inverter modulation was developed [12]. This technique named *Space Modulation Profiling (SMP)* carries out real-time compensation using a pre-determined envelope of the 'un-desired' harmonic distortion signals (multiples of the fundamental frequency). The harmonics due to the saturation saliency and the inverter distortions are removed from the demodulated HF currents using a pre-loaded profile for the direct position signal axis and a similar profile for the quadrature axis. The profile is recorded for rated flux and different loads w.r.t the stator current angle. Fig. 4 shows how the HC or SMP compensation is added to the HF currents in the HF frame before these are used for the rotor angle calculation.

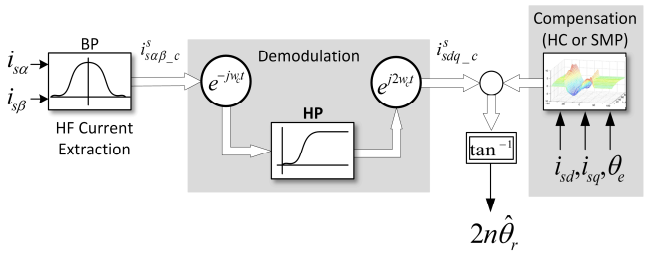

Fig. 4 Structure for Demodulation and Rotor Position Estimation using HF Injection.

In the case of rotor flux tracking, such as in a PMSM, a similar HF demodulation technique can be applied. The nonlinear effects of the inverter such as dead time and device voltage drop, can be compensated using an SMP table as above. For a PMSM the signal-injection method will yield a flux saliency and in the case of the SM-PMSM type, as explained in section 2.3, a phase correction must be applied to account for the shift of the saturation saliency due to the stator current magnitude. This is shown in Fig. 5 where the phase-correction curve has to be pre-determined using a commissioning process. In [14] it was reported that for a six-pole surface mount 4kW PMSM the saliency tends to orient with the stator flux rather than the rotor position. It was also reported that effects of the inverter nonlinearities on the injection signals may also contribute to the saliency shift.

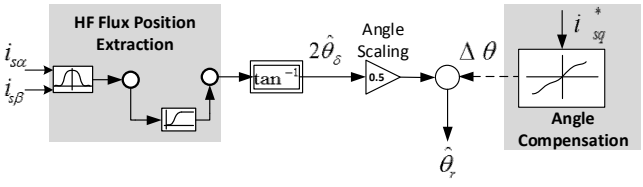

Fig. 5 Saliency Orientation Shift Compensation (Flux Position Tracking).

2.5 Pulsating HF Injection

Another injection scheme for sensorless control [15] makes use a fluctuating (pulsating) HF signal (ω_c) applied on the estimated rotor dq-axis. The technique makes use of a measurement axis purposely displaced by 45 degrees from the dq-axis as shown in Fig. 6. The advantage of the pulsating injection over the rotating injection is that it generates less torque ripple, vibrations and noise.

The injected voltage in the estimated rotor dq-frame is given by:

$$u^{\hat{r}}_{sdq\_c} = U_c(\cos\omega_c t) + j0 \quad \ldots\ldots(5)$$

Applying such HF injection to a machine which experiences a magnetic saliency (e.g. $Ld \neq Lq$ for an IPMSM) will result in saliency dependent HF currents. By tracking the resulting HF current on the measurement axis and applying the mathematical operations shown in Fig. 7, the error resulting between HF current amplitudes is proportional to the angle error, '$\Delta\theta$', between the control axis and the flux position (Fig. 6). This error is used as input for the PI based correction controller which estimates the speed so as to make the angle error zero thus aligning the estimated and real rotor frame.

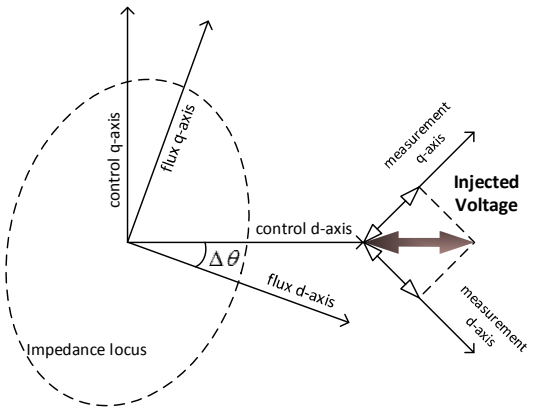

Fig. 6 Pulsating Carrier Injection Method Measurement Axis.

In [15], the author shows successful implementation of this technique (in Hybrid operation) with IPMSMs rated from 400W up to 6kW used in various industrial applications such as lifts, compressors and injection molding electric drives. However it was pointed out that this particular method does not work reliably with all machines since a stable and prominent magnetic saliency is required for position tracking.

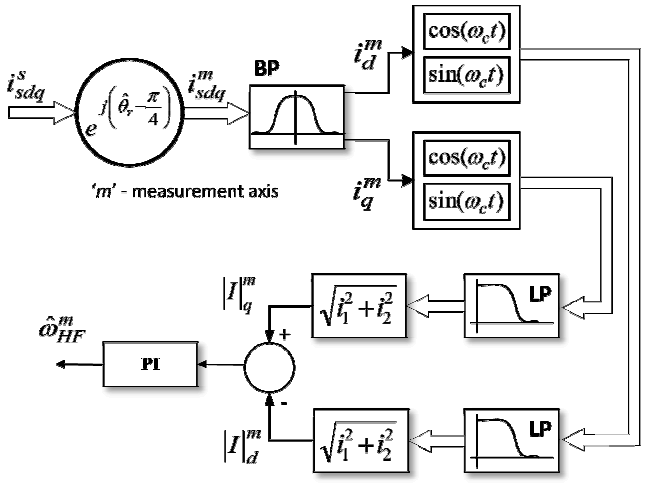

Fig. 7 Pulsating Signal Injection Technique.

2.6 Hybrid Operation

The HF injection techniques have been shown to operate successfully with most types of asynchronous and synchronous machines which experience a certain amount of saliency. The methods yield position and speed estimation at zero and low speed including zero stator frequency. However, there are disadvantages attributed to injection, namely:

1. increased torque ripple, losses and acoustic noise and,
2. the additional voltage required to inject the signal could possibly limit the maximum output voltage of the inverter during higher operating speeds.

For sensorless control it is recommendable to use injection methods only at zero and low speeds and switch to a model based system above a certain threshold speed. Fig. 8 shows the concept of a hybrid speed estimator which makes use of the injection method only at speeds where the model based estimation fails. The contribution of the injection method is gradually phased out, usually by means of speed dependent weighting, until a speed is reached which ensures correct operation of the model based estimation.

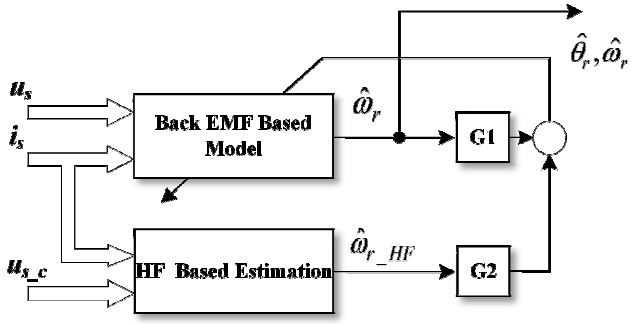

Fig. 8 Hybrid Concept for Wide Speed Range Sensorless Control.

In [14] and [15] hybrid techniques are implemented on a surface mount and an inset PMSM respectively. In [14], the hybrid system, which makes use of a continuous HF injection scheme, is applied on a six-pole 4kW commercial SM-PMSM. Fig. 9 shows how this system compares the estimated fluxes of the HF method and the model-based system to generate an error used to correct the model based system. The gain 'k' depends on the speed and is changed according to the estimated speed such that the injection estimate dominates the hybrid estimation at low speed. At higher speeds, 'k' is made smaller so that the voltage model dominates the hybrid estimation. Beyond a certain speed, 'k' is made zero. The feedback gain 'k1' is used to avoid that the flux estimator drifts whilst lowering the value of 'k', finally it shall be made sufficiently small to produce a negligible phase shift of the flux estimate at the upper frequencies. The author in [14] shows successful results of sensorless speed (±1500 rpm and 0 rpm) and position control at zero and full load operation.

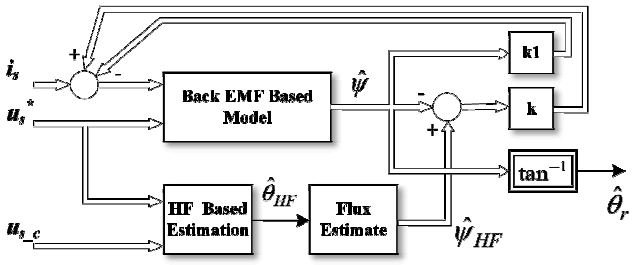

Fig. 9 Alternative Hybrid Concept for Wide Speed Range Sensorless Control.

In the hybrid system of Fig. 8, rather than the fluxes, the speed estimates are used for comparison [15]. The model based estimator is fed with an estimated speed feedback from both the HF-based speed estimation and that of the model based voltage model. In this case pulsating HF injection is used. The weightings given to the two speed estimates are G1 and G2, these are regulated according to the estimated speed. As for the previous method this allows the HF estimation technique to increase its contribution at zero and low speeds.

3. Transient Injection for Tracking Saliencies

3.1 Tracking Current Response

Transient injection methods differ from HF injection methods in that changes in the saliency dependent machine impedance are detected by means of the current derivative response to repetitive transient excitation. One way of transient injection requires the modification of the fundamental PWM switching by insertion of short voltage pulses [1,3,18,19]. Other methods simply make use of the inherent pulses already present in the PWM switching thus requiring no or little modification of the fundamental PWM pulses [10,20,21,22,24,26]. Recently other methods employing the switching harmonics themselves as a means of 'continuous' PWM harmonic injection [27] were also proposed and shall be discussed.

It can be shown that transient excitation affects mainly the leakage inductance since the transient flux component does not penetrate fast enough to establish mutual flux linkages [15]. By measuring the current derivative (CD) for a given voltage transient, the transient impedance can be determined. One of the main challenges is the type of sensor to be employed for measuring the resultant current derivative. If this is computed by use of standard current sensors the measurements shall suffer from poor transient response, sensitivity and noise. In this respect Rogowski coils are the most commonly used sensors for current derivative measurement since they yield a direct measurement of the derivative. However other CD sensors have been proposed such as the in-line mutually coupled ferrite sensors in [22] whose secondary voltage is proportional to the primary's current derivative (Fig. 17). Another limiting factor of current derivative measurement based methods is due to the settling time of the sensor, which is determined both by the transient response of the sensor and the machine's parasitic components [18]. This time is crucial in determining the time required between consecutive current samples. It has been reported that when comparing the performance of Rogowski coils to that of standard sensors, the former obtain shorter settling times [20]. The advantage of having such fast sensors is that they allow for shorter transient voltage injection widths during the fundamental PWM switching. Recently an oversampling technique has been proposed [20, 30], where rather than sampling once per PWM period, the current is sampled with maximum ADC frequency. Making use of a technique, such as the least squares linear regression, the current slope can be accurately calculated, moreover, since the mathematical operations are not very complex, this technique could easily be implemented on an FPGA [30].

The sections below shall discuss selected transient injection techniques.

3.2 Zero Sequence Current Derivative Method

The Zero Sequence Current Derivative (ZSCD) method of position estimation involves applying voltage test vectors corresponding to six non-zero switching states of a voltage source inverter [18]. The test vectors are of short duration (12-15µs) and are chosen from the vectors in Fig. 10. They are applied in equal and opposite pairs over one PWM cycle and will have no effect on the fundamental excitation of the machine. In [18] and [19] this method of transient injection was applied to a delta-connected induction machine. For every test voltage vector corresponding phase currents, as well as their zero sequence component, are set up in the machine. For a delta-connected machine the ZSC is given by the instantaneous sum of the three phase currents. To measure this, a single non-integrating Rogowski coil was wound on the start and end windings of the machine to detect the ZSCD.

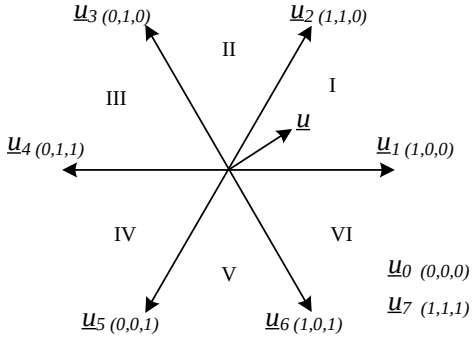

Fig. 10 Space Vector Definitions.

To detect a saliency dependent change in inductance test voltage vector pairs, ($\underline{u}_1$, $\underline{u}_4$), ($\underline{u}_3$, $\underline{u}_6$) and ($\underline{u}_5$, $\underline{u}_2$) are applied over successive PWM cycles and the ZSCD is sampled after every vector application. Sampling the ZSCD for each test vector pair gives a three phase system of "position" signals:

$$p_a = \frac{di_{s\_0}^{u_1}}{dt} or \frac{di_{s\_0}^{u_4}}{dt} \quad p_b = \frac{di_{s\_0}^{u_3}}{dt} or \frac{di_{s\_0}^{u_6}}{dt} \quad p_c = \frac{di_{s\_0}^{u_5}}{dt} or \frac{di_{s\_0}^{u_2}}{dt} \quad ...(6)$$

For an induction machine, these are defined by:

$$\begin{aligned} p_a &= k\left(\Delta l_{s\sigma\_sat}\cos(2\omega_e t - 4\pi/3) + \Delta l_{s\sigma\_RS}\cos(n\omega_r t - 4\pi/3 + \phi)\right) \\ p_b &= k\left(\Delta l_{s\sigma\_sat}\cos(2\omega_e t - 2\pi/3) + \Delta l_{s\sigma\_RS}\cos(n\omega_r t - 2\pi/3 + \phi)\right) \quad .....(7) \\ p_c &= k\left(\Delta l_{s\sigma\_sat}\cos(2\omega_e t) + \Delta l_{s\sigma\_RS}\cos(n\omega_r t + \phi)\right) \end{aligned}$$

where, k is a constant dependent on the DC link voltage.

Equation (7) represents a three phase system (p_a, p_b, p_c) of flux and rotor angle dependent signals which can be transformed to a 2-phase system (p_α, p_β). The two phase position signals can be resolved to yield the position angle according to which saliency is being tracked [19]. The terms in (7) are dependent both on machine saturation and on rotor slotting induced saliency. It is noted that (7) is ideal; in practice other harmonics will exist arising from other non-linear effects as explained in section 2.4. Since the separation of the different harmonic components of (7) cannot be done using real-time filtering a SMP-based method has to be used to obtain clean positions signals for rotor position estimation.

The ZSCD technique was implemented in practice on two types of induction machines [19], one with negligible rotor slotting harmonics and another with a pronounced rotor slotting effect. The first machine, which is more representative of commonly found IMs, was an 11kW 4-pole machine. The injection technique was used to track the "saturation" induced saliency to obtain rotor flux position. The second machine was a 30kW, 4-pole induction machine with open unskewed rotor slots with an optimum rotor slot number. In this case the rotor slot saliency was tracked from which rotor flux position and/or the rotor position may be obtained. Fig. 11 shows the 11kW machine's equivalent two phase position signals corresponding to (7) with and without application of SMP compensation. These are used to compute the machine's flux angle for rotor flux orientation. Fig. 12 shows the sensorless operation of the 30kW induction motor at zero speed and at zero fundamental frequency excitation achieved by operation at a reverse speed equal to the slip speed. In [19], experimental results of sensorless torque control are shown for the 11kW machine at zero/low speed operation, whilst sensorless speed and position control is shown for the 30kW machine. For both motors, results are carried out for no-load and rated load conditions.

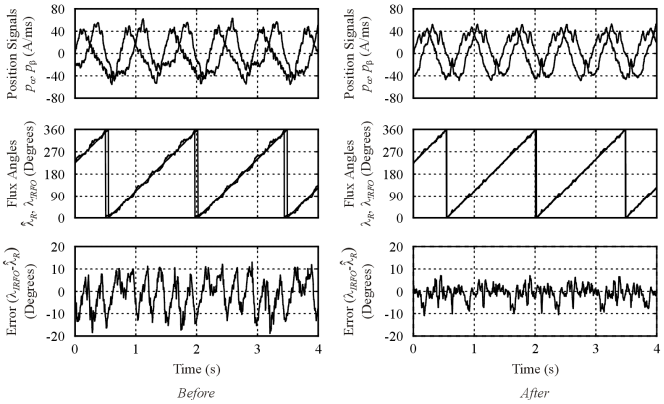

Fig. 11 Harmonic decoupling at 50% torque, zero speed: Top: position signals (p_α, p_β), Middle: Flux angles and Bottom: Flux angle error *before* and *after* compensation.

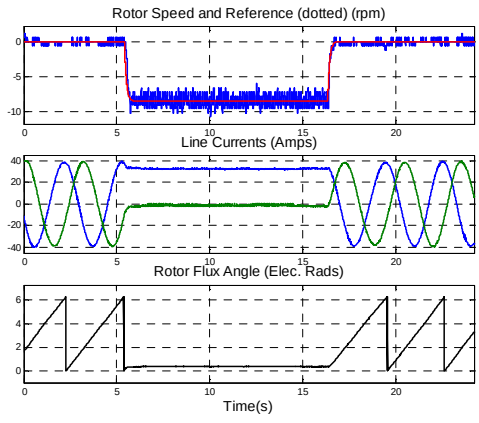

Fig. 12 Sensorless Speed Control at -8.5 rpm with 40% load application reducing fundamental frequency to 0Hz.

Although this method shows reliability and robustness at low/zero speed, the additional test vectors introduce extra losses and can also limit the fundamental voltage at higher speeds. Section 4 will discuss alternative sensorless techniques which are aimed at mitigating such issues.

3.3 Arbitrary Injection Scheme for Current Derivative based Saliency Detection

In [21] the authors propose a position extraction scheme that is independent of the type of injection, and hence applicable to different injection techniques. The algorithm only requires the presence of a current derivative, which can be obtained in different ways. The current derivative is expressed as the sum of two terms, one dependent on the mean admittance and the other dependent on the rotor position. By estimating the former, termed the isotropic current response, the term dependent on the rotor position can be extracted. Different combinations for extracting the position information are proposed [21,30], with the intent of extending the technique to the whole speed range. An additional injection is introduced in the low and medium speed range and the resulting current derivative is measured [21]. The injection is then switched off in the high speed range and the current derivative resulting from the discrete PWM switching is used for the position detection [30]. The same information measured for the position detection is used to estimate the mean admittance, which is required for the estimation of the isotropic current response.

As shown in (2), when machine saliencies are present, the inductance can be expressed in terms of a constant part and a saliency dependent part. In [21], it is shown that if the stator admittance for a salient PMSM is expressed in a constant mean part Y_Σ and a salient part Y_Δ, that is a function of the rotor position λ, then even the resulting current derivative can be expressed in terms of these two as follows:

$$\frac{d}{dt}\left(i_s^S\right)=Y_\Sigma\left(u_s^S-Ri_s^S-u_{bemf}^S\right)+Y_\Delta S(\lambda)\left(u_s^S-Ri_s^S-u_{bemf}^S\right) \quad \text{.....(8)}$$

where, $Y_\Sigma=\frac{Y_d+Y_q}{2}$, $Y_\Delta=\frac{Y_d-Y_q}{2}$

and $S(\lambda)=\begin{bmatrix}\cos(2\lambda) & \sin(2\lambda)\\ \sin(2\lambda) & -\cos(2\lambda)\end{bmatrix}$.

The first term on the RHS of (8) is termed the *isotropic current response* as it follows the direction of the voltage and depends on Y_Σ. The second term depends on Y_Δ and is correlated with the position information. Estimation of the isotropic current response allows the extraction of the position information from (8). The actual stator current progression resulting from the application of a voltage can be obtained from the difference between two consecutive current measurements as shown in Fig. 13. Considering the applied voltage and assuming knowledge of the other voltage terms and Y_Σ, the isotropic current progression can be estimated using:

$$\Delta i_{s\Sigma}^S[n]=Y_\Sigma\left(u_s^S[n-1]-Ri_s^S[n-1]-u_{bemf}^S[n-1]\right)T_s \quad \text{.....(9)}$$

where T_s is the sampling period.

The position information can be extracted from:

$$p[n]=\Delta i_s^S[n]-\Delta i_{s\Sigma}^S[n] \quad \text{.....(10)}$$

In Fig. 13, this position estimate is already available after the calculation of the first actual current derivative and the isotropic current derivative. However the authors in [21] propose a method which eliminates the influence of the isotropic model on the stator resistance, the PM flux and the rotor speed. This is done by differentiating the real and isotropic current derivatives as shown in the second stage of Fig. 13. An expression in terms of only the imposed stator voltage components can be obtained by considering the difference between two consecutive isotropic current progressions, $\Delta(\Delta i_{s\Sigma}^{S})[n]$, rather than the current progressions themselves. The rotor flux angle can then be calculated from (Fig. 13):

$$\hat{\lambda} = \frac{1}{2}\tan^{-1}\left(\frac{\Delta u_{\alpha}^{s}\Delta p_{\beta} + \Delta u_{\beta}^{s}\Delta p_{\alpha}}{\Delta u_{\alpha}^{s}\Delta p_{\alpha} - \Delta u_{\beta}^{s}\Delta p_{\beta}}\right) \quad \text{.....(11)}$$

where $\Delta \boldsymbol{u}_{\alpha\beta}$ is the change in the applied voltages when the current derivatives are sampled.

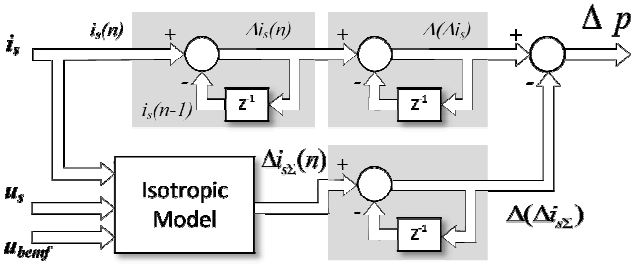

Fig. 13 Extraction of Position Dependent term '$\Delta \boldsymbol{p}$' with measured and estimated (isotropic) current derivatives.

In order to establish the response of the required current derivatives, a rectangular high frequency signal at half the PWM frequency, rotated with a step size of integer functions of 2π, is used in [21]. Experimental results on a 1.57kW, 3000rpm surface mount PMSM are shown. In [21] speed transients from 0 rpm to 600rpm with zero and 60% load are shown. Steady state operation at 100rpm, at zero and rated load is also reported.

The above assumes that the low frequency terms remain constant for consecutive sampling cycles. This will hold up to medium speed and will hence restrict the use of the proposed scheme for higher speeds. In order to extend the application range, an extension of the above method is proposed in [30]. Rather than constant, the low frequency terms are assumed to show a linear variation and their effect can be decoupled by combining two consecutive differences in the current progression. Since voltage injection limits the excitation range for the fundamental control [30], the additional injection is turned off for higher speeds. The current derivatives resulting from the discrete PWM switching are used instead. This requires the extension of the current measurement such that the current progression for each discrete vector is measured. In [30], experimental results for a 0.678kW, 3000rpm SM-PMSM show a speed transient up to 3800rpm at no load and a load step up to 1.5 nominal torque at 3200rpm.

The estimation of the anisotropic current response depends on the mean stator admittance Y_{Σ}, which despite shown as constant in the equations above, is expected to show some variation especially at high load. The authors of [21,30] have proposed an offline procedure whereby a lookup table, referenced by the machine torque is used for compensation. Moreover to further reduce the dependency on machine parameters, it was even proposed to estimate Y_{Σ} online. Various solutions for estimating Y_{Σ} values are proposed in [21,30].

The proposed arbitrary injection demodulation scheme can be applied for different forms of injection, allows operation in the high speed range with no additional injection and is applicable even to small saliency machines. As it uses a direct angle extraction, it allows high bandwidth rotor position estimation [21]. The method requires a precise estimation of the mean admittance Y_{Σ} as the position information is extracted from the difference of two signals with significantly higher magnitudes and could be susceptible to noise.

4. PWM-Based Injection for Tracking Saliencies

One of the first techniques of PWM-based sensorless position estimation without additional signal injection was reported in [9,10]. This method was based on the separation of the real time current into a fundamental (average) component and a transient (harmonic) component. The authors showed that for this technique to work conventional sinusoidal PWM could not be used and a novel PWM generation method, making use of the zero voltage vectors, was introduced. By measurement of the resultant harmonic currents and knowledge of the harmonic voltage component, the rotor position dependent machine inductance matrix and consequently the rotor position were computed every PWM cycle. This technique was successfully implemented on a low power IPM machine which exhibited a large saliency.

This section will review methods which employ the inherent PWM switching to serve as the excitation mechanism. These methods measure the resulting current transient response produced by standard (or slightly modified) PWM excitation [22,23,24,26]. Although no additional signal injection or separate test vector is required, slight modification of the PWM by extended modulation or edge shifting [24] could be required.

4.1 Edge Shifting of Standard SVPWM

In section 3.2 a technique was shown where test vectors of a predetermined fixed duration where added to the fundamental PWM. Recently, techniques which use the switching states inherently present in the fundamental PWM waveform were developed [22,23,24,25,26]. However the duration of these inherent 'test' vectors is determined by the PWM operation and there can be instances when these are very short (Fig. 14(a)). Similarly to the ZSCD method, these techniques are based on the direct measurement of the line current derivative, which imposes a minimum test vector duration (usually between 5-25μs, depending on the machine type), to allow for HF common mode and differential mode current oscillations to die away prior to current sampling. (Rogowski coils are normally employed for *di/dt* measurement). The most critical cases where the application time of one voltage vector becomes too short are:

1. low-speed operation: when application time of active voltage vector is low;
2. transition of space voltage vector between sectors: the application time of an active voltage vector becomes very low (even zero) at each sector transition.

To guarantee a minimum vector duration modification of the PWM switching is required. In [23] an extended modulation principle is used to lengthen the vectors without changing the fundamental PWM operation. In [24] a similar approach was implemented, however with the added advantage that unlike [23], the resulting voltage transients are of half the magnitude (equal to the DC-link voltage). The short duration issue of "narrow vectors" is mitigated by an edge shifting method applicable at all operating frequencies including high, low, and zero frequencies. Fig. 14 (a) shows the operation when the inherent 'test' vectors are short and below the allowable minimum duration for successful current measurement. Fig. 14 (b) shows how the elegant technique in [24] extends the duration of the 'test' vector by simple edge shifting which will increase the duration of the u_1 and u_2 vectors but at the same time create new vectors u_4 and u_7 which are opposite to the former pair and of the same duration of the increase in duration of the former pair. Thus the fundamental PWM waveform shall remain unchanged.

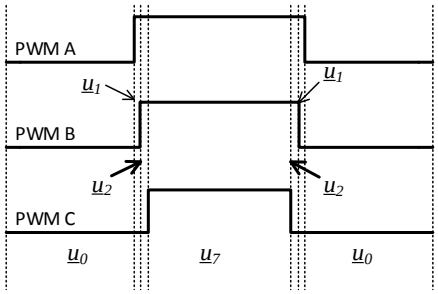

(a) Standard PWM switching with short u_1 and u_2 vectors.

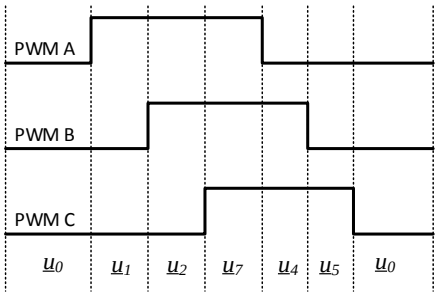

(b) Shifting of SVPWM sequence for small u_1 and u_2 vectors by introduction of u_4 and u_7 vectors.

Fig. 14 SVPWM Edge Shifting Technique.

The mathematical relationship between the inherent 'test' vectors and the saliences present in ac machines is similar to that introduced in section 3.2. However in this case the resulting three phase position dependent signals are calculated every PWM period by making use of *di/dt* samples following a combination of a vector pair selected from {(u_1, u_0), (u_2, u_0), (u_3, u_0), (u_4, u_0), (u_5, u_0), (u_6, u_0)}for each of the SIX sectors (Fig. 10). The processing of the signals is different due to the presence of constants which need to be eliminated. The author of [24] applies this technique for sensorless speed and position operation of a 30kW Δ-connected IM exploiting the slotting anisotropy of an open-slot cage rotor, however the technique can also be applied to star connected IMs and PMSMs which exhibit a trackable saliency.

In [25] and [26] the principle of this technique is applied also to a surface and an interior permanent magnet synchronous machine respectively. In [26], the above method is extended as shown in Fig. 15, where four samples are taken within one PWM period. The mathematical method adopted then makes use of the *di/dt* samples following two vector pairs to allow for saliency position tracking at both low and high speeds. The technique is used with a fractional power high speed IPMSM. In [26], the author shows that even at high speeds accurate rotor position tracking is made possible by assuming linear variation of position within one PWM period and applying an interpolating mechanism between measurements from the sample pairs (1,2) and (3,4) of Fig. 15.

One drawback of the edge shifting technique is the effect that it has on the symmetry of the fundamental PWM waveform. If synchronised sampling is used for fundamental control it shall be affected and a compensation strategy is required.

The advantage of methods which utilise 'inherent' PWM switching is that they do not introduce additional losses of the magnitude of the techniques which use extra injection. The machine experiences only a minor increase in injection losses which occurs when PWM switching modification is required during short vectors. However, depending on the type of PWM modification applied, there can be increased common mode currents and even high voltage stresses caused by transitions of twice the DC link voltage in some cases.

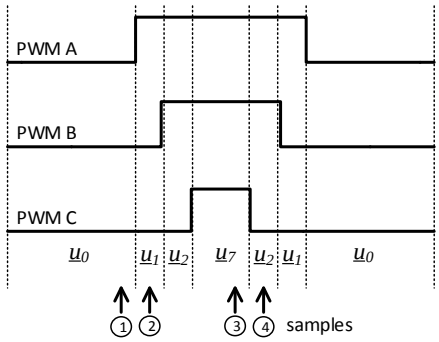

Fig. 15 Sampling of four CDs within one PWM period.

4.2 Zero Sequence Carrier Injection

Another sensorless technique for PMSMs that utilises also the current derivative to retrieve rotor position information from the stator inductance variation is presented in [22]. The response to the zero sequence voltage vectors $\underline{u}_0$ ($\mathbf{u_{000}}$) and $\underline{u}_7$ ($\mathbf{u_{111}}$), that occur twice per PWM cycle (Fig. 16) is analysed by dedicated current derivative sensors. Two sensors, shown in Fig. 17, are used to provide directly the zero sequence current derivative position dependent vector information in the $\alpha\beta$ frame. This provides the rotor flux position information in a similar way to that discussed in section 3.2.

In order to allow for a sufficient zero sequence current the motor star point $\boldsymbol{N}$ is connected to the midpoint $\boldsymbol{O}$ of the DC link. The current flowing between these two points is limited by the $\boldsymbol{L_f}$ and $\boldsymbol{C_f}$ filter impedance. The filter $\boldsymbol{L_f}$ and $\boldsymbol{C_f}$ values are particularly adjusted to limit any low frequency currents that may increase additional losses, but allow sufficient current ripple for the zero sequence current derivative measurement during the voltage zero vectors.

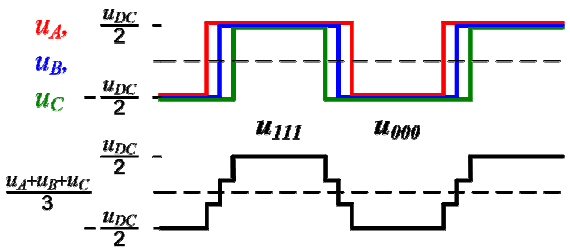

Fig. 16 Phase and Zero Sequence VSI output voltages.

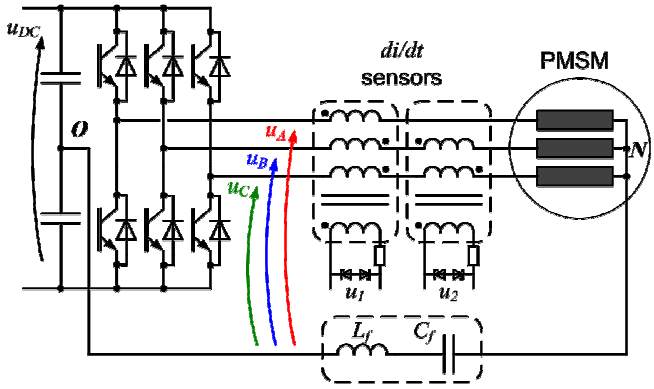

Fig. 17 Phase and zero sequence VSI output voltages.

In [22], the method shows results of sensorless speed and position control for a surface mount PMSM at no-load and half rated load. In [22], the author shows that in the case of motors with high saliences, a simple compensation method is required in order to compensate distortions due to the high saliency. A disadvantage of this method is that it requires additional hardware in the form of an impedance between the machine star point and the inverter DC link mid-point.

5. Using PWM Harmonics for Saliency-based Sensorless Control

In [28] it was shown that the natural switching related harmonics contained in PWM voltages can be used for the sensorless control of induction machines. Hence no additional test signal injection is required and the fundamental control of the drive will be unaffected. The principle of saliency detection is very similar to standard high frequency injection methods. The major difference here is that no additional HF is injected into the machine, instead part of the inherit PWM ripple is used as HF signal. For the implemented sensorless drive the 2nd PWM carrier harmonic is filtered out of the measured voltages and currents and demodulated. The division of the resulting demodulated HF voltage and current vectors $\underline{u}'_{PWM2}$ and $\underline{i}'_{PWM2}$ gives the vector $\underline{z}'_{PWM2}$ which provides information about the HF stator impedance. This process is shown in Fig. 18.

The rotor position information is extracted from $\underline{z}'_{PWM2}$ following compensation for offset, saturation modulation and inverter disturbances. For this a complex pre-commissioned look up table (LUT) dependant on the fundamental stator current vector (position and magnitude) and the HF stator current vector is required [28].

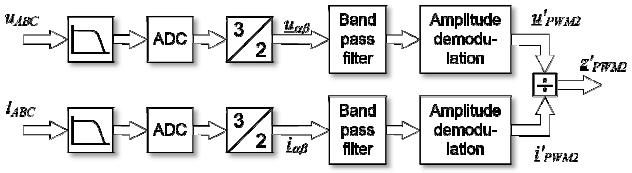

Fig. 18 Extraction of $\underline{z}'_{PWM2}$ Impedance from measured PWM frequency voltages and currents.

A standard 5.5kW 2-pole off-the-shelf induction motor with 32 rotor slots was used for verification of the method and its suitability for position estimation via the rotor slotting effect. The motor showed a low stator impedance rotor bar modulation of only 1 to 1.5%. The modulation due to saturation and inverter non-linearity were of comparable magnitudes. Therefore the decoupling of the desired signal for the rotor position estimation from the other distorting effects is a critical task and a LUT compensation scheme needs to be implemented to extract only the desired rotor bar modulation.

The extracted mechanical rotor position allows closed loop sensorless torque, speed and position control. Fig. 19 and Fig. 20 show results of the sensorless IM drive in speed and position control. Plot (a) shows the estimated and measured mechanical rotor position and plot (b) shows the stator current vector components in the estimated dq^e frame used for vector current control. Fig. 19 shows speed control operation at ±60rpm with a load varying from half to full rated. Fig. 20 shows position control for ± 1 mechanical revolution at half and full rated load.

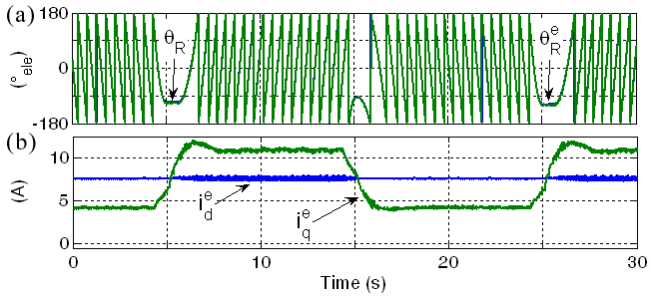

Fig. 19 Results of sensorless speed control (a) Measured mechanical rotor position θ_R and estimated rotor position θ^e_R, (b) i^e_{dq} current components of the sensorless controlled drive.

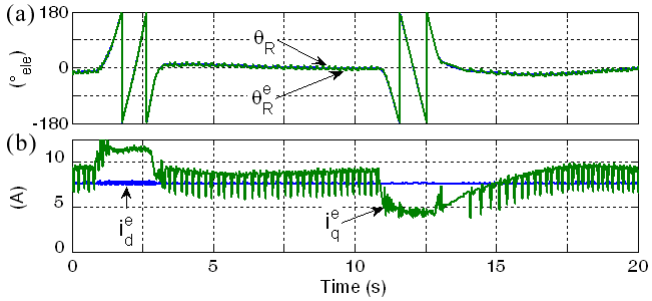

Fig. 20 Results of sensorless position control. (a) Measured mechanical rotor position θ_R and estimated rotor position θ^e_R, (b) i^e_{dq} current components of the sensorless controlled drive.

This harmonic based method of estimation has shown sensorless operation at low/zero speed and excitation frequency, however for correct operation it requires a complex predetermined machine

specific compensation LUT which is needed for decoupling the additional modulation caused by saturation and inverter effects.

6. Conclusions

Speed and position estimation for sensorless control of AC machines can be carried out using either model based systems or injection based systems or a combination of the two. Research has shown that sensorless control for asynchronous and PM synchronous machines can cover all operating speeds and fundamental excitation frequencies by using either hybrid systems or in some cases even saliency detection techniques devised to work at low and higher speeds.

For operation at low and zero speed, injection based techniques have to be applied since model based estimation is unreliable. The injection techniques can be of the transient or continuous injection type and work by tracking a machine saliency for rotor position or flux position estimation. The performance of the injection based technique is highly dependent on the machine's saliency. Thus the development of novel motor designs taking into account integration with saliency detection techniques could facilitate the implementation of these injection based sensorless methods.

Recently new methods to detect saliencies by making use of the inverter's inherent PWM switching have been introduced. This has the advantage of reducing extra injection losses and removing the limitations imposed by the injection on the fundamental voltage itself. However there are instances where slight modification of the PWM pulses is required to produce sufficient duration of transient excitation for proper saliency detection. One drawback of PWM-based sensorless techniques and even transient injection based techniques is that usually they require additional sensor/s for sampling of the transient current response.

Recent research directed towards using the PWM switching or its inherent high frequency harmonic generation without undergoing any modification has also been carried out. The main advantage is that no injection or PWM modification is required. The move towards techniques injecting lower strength signals or no additional test signals have made the compensation crucial for the reliable operation of sensorless drives. The complexity of the necessary compensating signals might limit the attractiveness of non-model based sensorless drives for industrial applications. However through the development of novel motor designs and auto commissioning compensation techniques the implementation of these sensorless methods will facilitate their widespread use in industry.

References

1. M. Schrödl, "Sensorless Control of AC Machines at Low Speed and Standstill Based on the INFORM Method," IEEE IAS Annual Meeting, San Diego, USA, Oct. 1996, Vol. 1 pp. 270-277.
2. J. Ha and S. Sul, "Sensorless Field Orientation Control of an Induction Machine by High Frequency Signal Injection," IEEE Trans. Ind. Appl., Vol. 35, No. 1, Jan/Feb 1999, pp. 45-51.
3. J. Holtz, "Sensorless Position Control of Induction Motors - An Emerging Technology," IEEE Trans. Ind. Electron., Vol. 45, No. 6, Dec. 1998, pp. 840-852.
4. P.L. Jansen and R.D. Lorenz, "Transducerless Position and Velocity Estimation in Induction and Salient AC Machines," IEEE Trans. Ind. Appl., Vol.31, No.2 , March/April 1995, pp. 240-247.
5. P.L. Jansen and R.D. Lorenz, "Transducerless Field Orientation Concepts Employing Saturation Induced Saliencies in Induction Machines," IEEE IAS Annual Meeting, Vol. 1, 1995, pp. 174-181.
6. J. Cilia, G.M. Asher, K.J. Bradley and M. Sumner, "Sensorless Position Detection for Vector Controlled Induction Motor Drives using an Asymmetric Outer-Section Cage," IEEE Trans. Ind. Appl., Vol. 33 No. 5, Sep/Oct 1997, pp. 1162-1169.
7. M.Corley, R.D. Lorenz, "Rotor position and velocity estimation for a salient-pole permanent magnet synchronous machine at standstill and high speeds," IEEE Trans. Ind. Appl., Vol. 33 No. 4, 1998, pp. 784-789.
8. M.W. Degner and R.D. Lorenz, "Using multiple saliencies for the estimation of flux, position, and velocity in AC machines," IEEE Trans. Ind. Appl., Vol. 34, Sep/Oct 1998, pp. 1097-1104.
9. Ogasawara, S. ; Akagi, H., "An Approach to Real-Time Position Estimation at Zero and Low Speed for a PM Motor Based on Saliency", IEEE Trans. Ind. Appl., No. 1, Vol. 34, Jan/Feb. 1998, pp. 163-168.
10. Ogasawara, S. ; Akagi, H., "Implementation and position control performance of a position-sensorless IPM motor drive system based on magnetic saliency", IEEE Trans. Ind. Appl., No. 4, Vol. 34, July/Aug. 1998, pp. 806-812.
11. N. Teske, G. M. Asher, M. Sumner, and K. J. Bradley, "Encoderless position estimation for symmetric cage induction machines under loaded conditions," IEEE Trans. Ind. Appl., No. 6, Vol. 37, Nov/Dec. 2001, pp. 1793-1800.
12. N. Teske, G. M. Asher, M. Sumner, and K. J. Bradley, 'Analysis and Suppression of High-Frequency Inverter Modulation in Sensorless Position-Controlled Induction Machine Drives', IEEE Trans. Ind. Appl., No. 1, Vol. 39, Dec. 2003, pp. 10-18.
13. M.W. Degner and R.D. Lorenz, "Position Estimation in Induction Machines Utilizing Rotor Bar Slot Harmonics and Carrier-Frequency Signal Injection," IEEE Trans. Ind. Appl., May/June 2000, Vol. 36, No. 3, pp. 736-742.
14. C. Silva, G. M. Asher and M. Sumner, "Hybrid Rotor Position Observer for Wide Speed-Range Sensorless PM Motor Drives Including Zero Speed," IEEE Trans. Ind. Appl., Vol. 53, No. 2, April 2006, pp. 373-378.
15. S. Sato, H. Iura, K. Ide, and, S.-K. Sul, "Three years of industrial experience with sensorless IPMSM drive based on high frequency injection method," 2nd Symposium on Sensorless Control of Electrical Drives, Sep 2011, Birmingham, UK, CDROM.
16. P. Garcia; F. Briz,; D. Raca,; R.D Lorenz, 'Saliency-Tracking-Based Sensorless Control of AC Machines Using Structured Neural Networks,' IEEE Trans. Ind. Appl., Vol. 43 No. 1, Jan/Feb 2007, pp. 77-86.
17. J.Holtz, 'Sensorless Control of Induction Machines — With or Without Signal Injection?,' IEEE Trans. Ind. Electron., Vol. 53, No. 1, Dec 2006, pp. 7-30.
18. C. Caruana, G. M. Asher and J. Clare, "Sensorless Flux Position Estimation at Low and Zero Frequency by measuring Zero-Sequence Current in Delta Connected Cage Induction Machines", IEEE IAS Annual Meeting, Salt Lake City, 2003, CDROM.
19. Spiteri Staines, C.; Caruana, C.; Asher, G.M.; Sumner, M., "Sensorless control of induction Machines at zero and low frequency using zero sequence currents" IEEE Trans. Ind. Electron., Vol. 53, Issue 1, Feb. 2006, pp. 195 - 206.
20. P. Nussbaumer, T. M. Wolbank, "Using Switching Transients to Exploit Sensorless Control Information for Electric Machines," 2nd Symposium on Sensorless Control of Electrical Drives, Sep 2011, Birmingham, UK, CDROM.
21. D. Paulus, P. Landsmann and R. Kennel, "Sensorless Field- oriented Control for Permanent Magnet Synchronous Machines with an Arbitrary Injection Scheme and Direct Angle Calculation," 2nd Symposium on Sensorless Control of Electrical Drives, Sep 2011, Birmingham, UK, CDROM.
22. R. Leidhold, "Position Sensorless Control of PM Synchronous Motors Based on Zero-Sequence Carrier Injection," IEEE Trans. Ind. Electron., Vol. 58, No. 12, Dec 2011, pp . 5371-5379.
23. J. Juliet and J. Holtz, "Sensorless acquisition of the rotor position angle for induction motors with arbitrary stator windings," in Proc. IEEE IAS Annu.

Meeting, 2004, CDROM.

24. Q. Gao, G. Asher and M. Sumner and P. Makyš, "Position Estimation of AC Machines Over a Wide Frequency Range Based on Space Vector PWM Excitation," IEEE Trans. Ind. Appl., Vol. 43, NO. 4, July/Aug. 2007, pp. 1001-1011
25. Y. Hua, G. M. Asher, M. Sumner, Q. Gao, "Sensorless Control of Surface Mounted Permanent Magnetic Machine Using the Standard Space Vector PWM," in Proc. 42nd Industry Application Conference, IAS Annual Meeting, 2007, pp. 661-667.
26. S Bolognani, S. Calligaro, R. Petrella, and M. Sterpellone, "Sensorless control for IPMSM using PWM excitation: Analytical developments and implementation issues," 2nd Symposium on Sensorless Control of Electrical Drives, Sep 2011, Birmingham, UK, CDROM.
27. Y. Hua, M. Sumner, G. Asher ,Q. Gao and K. Saleh, 'Improved sensorless control of a permanent magnet machine using fundamental pulse width modulation excitation,' IET Electr. Power Appl., Vol. 5, Iss. 4, 2011, pp. 359-370.
28. R. Raute, C. Caruana, C. Spiteri Staines, J. Cilia, M. Sumner and G. M. Asher, "Sensorless Control of Induction Machines at Low and Zero Speed Using PWM Harmonics for Rotor Bar Slotting Detection," IEEE Trans. Ind. Appl., vol. 46, no. 5, Sep./Oct. 2010, pp. 1989-1998.
29. M. Schrödl, W. Staffler, M. Hofer, "Accuracy of the sensorless determined rotor position for industrial standard drives in the whole speed range," EPE '09, 13th European Conference Power Electronics and Applications, 2009, pp. 1-6.
30. P. Landsmann, J. Jung, M. Kramkowski, P. Stolze. D. Paulus and R. Kennel, 'Lowering Injection Amplitude in Sensorless Control by means of Current Oversampling.' 3rd Symposium on Sensorless Control of Electrical Drives, September 2012, WI, USA, CDROM.
31. D. Paulus, P. Landsmann and R. Kennel, "Saliency based field-oriented control for permanent magnet synchronous machines in the whole speed range," 3rd Symposium on Sensorless Control of Electrical Drives, Sep 2012, WI, USA, CDROM.

Cyril Spiteri Staines (Member) received the B.Eng.(Hons.) degree from the University of Malta in 1994, and the Ph.D. degree in Electrical Engineering from the University of Nottingham, 1999. In 1995, he joined the Faculty of Engineering, University of Malta as an Assistant Lecturer, where he became a Lecturer in 1999, Senior Lecturer in 2004, and Associate Professor in 2007. From 2003 to 2004, he was a Postdoctoral Researcher and Visiting Lecturer at the University of Nottingham. His research interests include sensorless AC motor drives and grid connection of renewable energy sources, in particular, for wind-energy systems. Prof. Spiteri Staines is a member of the IEEE, IET and IEEJ.

Cedric Caruana (Non-member) received the Ph.D. degree in electrical engineering from the University of Nottingham, Nottingham, U.K., in 2003. He was with Carlo Gavazzi (Malta) Ltd. and ST Microelectronics (Malta) Ltd. as a Process Engineer and Senior Test Engineer, respectively. He has been with the Faculty of Engineering, University of Malta, Msida, Malta, following receipt of the Ph.D. degree, where he is currently a Senior Lecturer. His main research interests are the control of ac drives, renewable energy conversion, electrical power systems, and energy efficiency. Dr. Caruana is a member of the IEEE and IET.

Reiko Raute (Non-member) started his education in electrical engineering with a vocational training as electronic process control engineer at EKO Stahl in Eisenhüttenstadt, Germany. He continued to study electrical engineering and at the University of Applied Science Jena. During his studies he visited the University of Nottingham and the University of Adelaide working on electric drive projects. In December 2009 he received his PhD degree from the University of Nottingham. After spending a few years working in industry, in 2013 he joined the Department of Industrial Electrical Power Conversion at the University of Malta.